

Collective modes and sum rules within nuclear density functional theory

Nobuo Hinohara

Center for Computational Sciences, University of Tsukuba, Japan
NSCL/FRIB, Michigan State Univ., USA



筑波大学
計算科学研究中心
Center for Computational Sciences



Outline

- ❑ finite amplitude method

- ❑ discrete collective states

- ❑ sum rules

- ❑ Nambu-Goldstone mode

- ❑ non-axial ($K \neq 0$) modes

Finite amplitude method: alternative to QRPA

QRPA equation (matrix formulation)

$$[\hat{H}', \hat{O}_\lambda^\dagger] = \omega_\lambda \hat{O}_\lambda^\dagger \quad \longleftrightarrow \quad \begin{pmatrix} A & B \\ B^* & A^* \end{pmatrix} \begin{pmatrix} X^\lambda \\ Y^\lambda \end{pmatrix} = \omega_\lambda \begin{pmatrix} X^\lambda \\ -Y^\lambda \end{pmatrix}$$

$$\hat{O}_\lambda^\dagger = \sum_{\mu\nu} X_{\mu\nu}^\lambda \hat{a}_\mu^\dagger \hat{a}_\nu^\dagger - Y_{\mu\nu}^\lambda \hat{a}_\nu \hat{a}_\mu$$

X, Y: amplitudes

ω : excitation energy

A, B: matrix elements from effective two-body interaction

computationally demanding calculation

- construction of the AB matrix / diagonalization

qp space truncation

- HFB cutoff (delta- pairing renormalization)

- QRPA two-quasiparticle cutoff (numerical reason)

efficient technique for QRPA

enables us to use QRPA for DFT optimization (T-odd etc.),
whole nuclear chart calculation

Which quantities do we need from QRPA?

(matrix) QRPA solutions

- eigenvalues: excitation energies
- eigenvectors: QRPA two-quasiparticle amplitudes (X,Y)

- giant resonances:**  original FAM
structure of the strength functions (smeared)
- collective low-lying states:**  complex-energy FAM
excitation energies, amplitudes of (several) discrete states
- sum rules:**  complex energy FAM
energies, strength functions of all excited states

Finite amplitude method (FAM)

linear response solution to QRPA
 frequency ω (of external field)
 fixed during iteration

Nakatsukasa et al., PRC76,024318(2007)

TDDFT equation

$$i \frac{\partial \hat{a}_\mu(t)}{\partial t} = [\hat{H}(t) + \hat{F}(t), \hat{a}_\mu(t)]$$

time-dependent
external field

oscillation of the quasiparticles

$$\hat{a}_\mu(t) = \{\hat{a}_\mu + \delta\hat{a}_\mu(t)\} e^{iE_\mu t},$$

induced field

$$\hat{H}(t) = \hat{H}_0 + \delta\hat{H}(t)$$

two-body

one-body

oscillation of densities

$$\rho(t) = \rho_0 + \delta\rho(t)$$

$$\kappa(t) = \kappa_0 + \delta\kappa(t)$$

one-body

$$h[\rho], \Delta[\rho, \kappa]$$

- weak time-dependent external field ($e^{i\omega t}$, $e^{-i\omega t}$)
- iterative solution
- one-body induced field not through two-body AB matrices
- easy implementation on top of existing mean-field codes

original FAM

Why the original FAM works only for resonances?

ω (freq. of external field) has to be complex

$$\frac{dB(\omega, F)}{d\omega} = \sum_{i>0} |\langle i | \hat{F} | 0 \rangle|^2 \delta(\omega - \Omega_i)$$

The response function from FAM

$$S(\hat{F}, \omega_\gamma) = - \sum_{\nu} \left\{ \frac{|\langle \nu | \hat{F} | 0 \rangle|^2}{\Omega_\nu - \omega_\gamma} + \frac{|\langle 0 | \hat{F} | \nu \rangle|^2}{\Omega_\nu + \omega_\gamma} \right\}$$



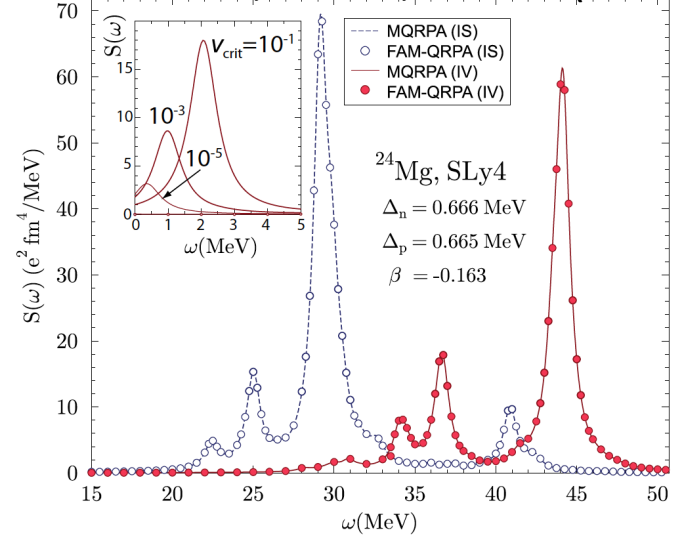
$$\frac{dB(\hat{F}, \omega)}{d\omega}(\omega_\gamma) = -\frac{1}{\pi} \text{Im} S(\hat{F}, \boxed{\omega + i\gamma}) = \frac{\gamma}{\pi} \sum_i \left\{ \frac{|\langle i | \hat{F} | 0 \rangle|^2}{(\Omega_i - \omega)^2 + \gamma^2} - \frac{|\langle 0 | \hat{F} | i \rangle|^2}{(\Omega_i + \omega)^2 + \gamma^2} \right\}$$

distribution smeared with Lorentzian

real ω : real $S(F, \omega)$, and $dB/d\omega=0$

width γ is always necessary

Stoitsov et al, PRC84, 041305 (2011)



FAM for discrete low-lying states

FAM equations $\left[\begin{pmatrix} A & B \\ B^* & A^* \end{pmatrix} - \omega \begin{pmatrix} 1 & 0 \\ 0 & -1 \end{pmatrix} \right] \begin{pmatrix} X(\omega) \\ Y(\omega) \end{pmatrix} = - \begin{pmatrix} F^{20} \\ F^{02} \end{pmatrix}$ Phys. Rev. C87, 064309 (2013)

$$\begin{pmatrix} X(\omega) \\ Y(\omega) \end{pmatrix} = - \left[\begin{pmatrix} A & B \\ B^* & A^* \end{pmatrix} - \omega \begin{pmatrix} 1 & 0 \\ 0 & -1 \end{pmatrix} \right]^{-1} \begin{pmatrix} F^{20} \\ F^{02} \end{pmatrix}$$

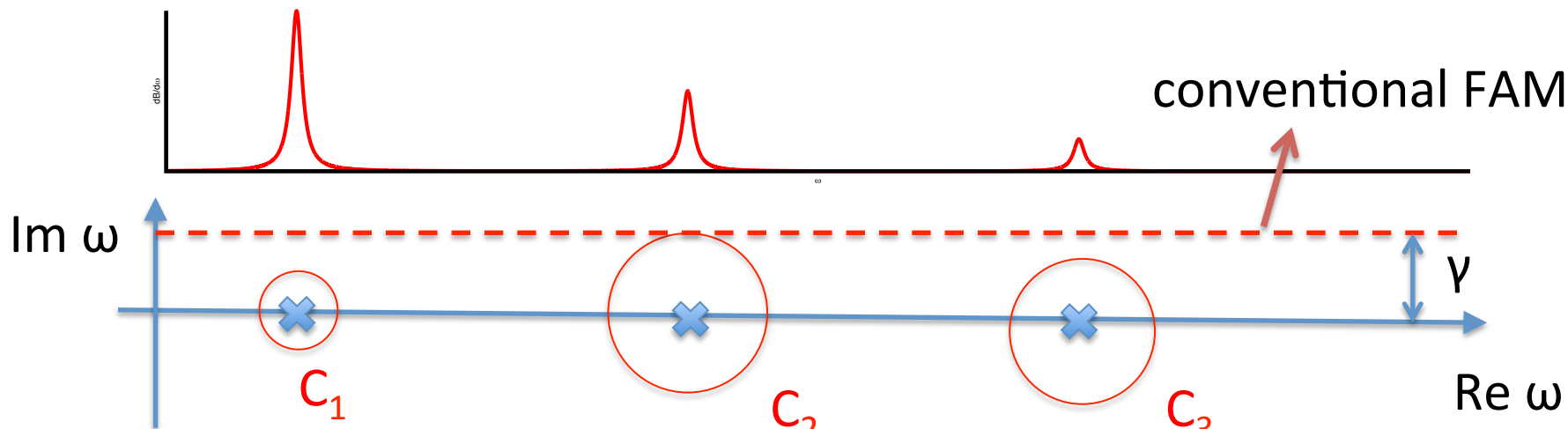
first-order poles at $\omega = \Omega_i$ (QRPA energies)

Contour integration

$$\frac{1}{2\pi i} \oint_{C_i} \begin{pmatrix} X(\omega) \\ Y(\omega) \end{pmatrix} d\omega = \langle i | \hat{F} | 0 \rangle \begin{pmatrix} X^i \\ Y^i \end{pmatrix}$$

$X(\omega), Y(\omega)$: FAM amplitudes

X, Y : QRPA eigenvectors



cf. solution of eigenvalue problem using contour integration

Sakurai and Sugiura J. Comp. App. Math 159, 119 (2003).

Numerical comparison with MQRPA

FAM code for K=0 developed in Stoitsov et al., PRC84, 041305 (2011)

^{24}Mg , oblate configuration (HFBTHO, SLy4) 5 oscillator shells
isoscalar/isovector monopole excitation

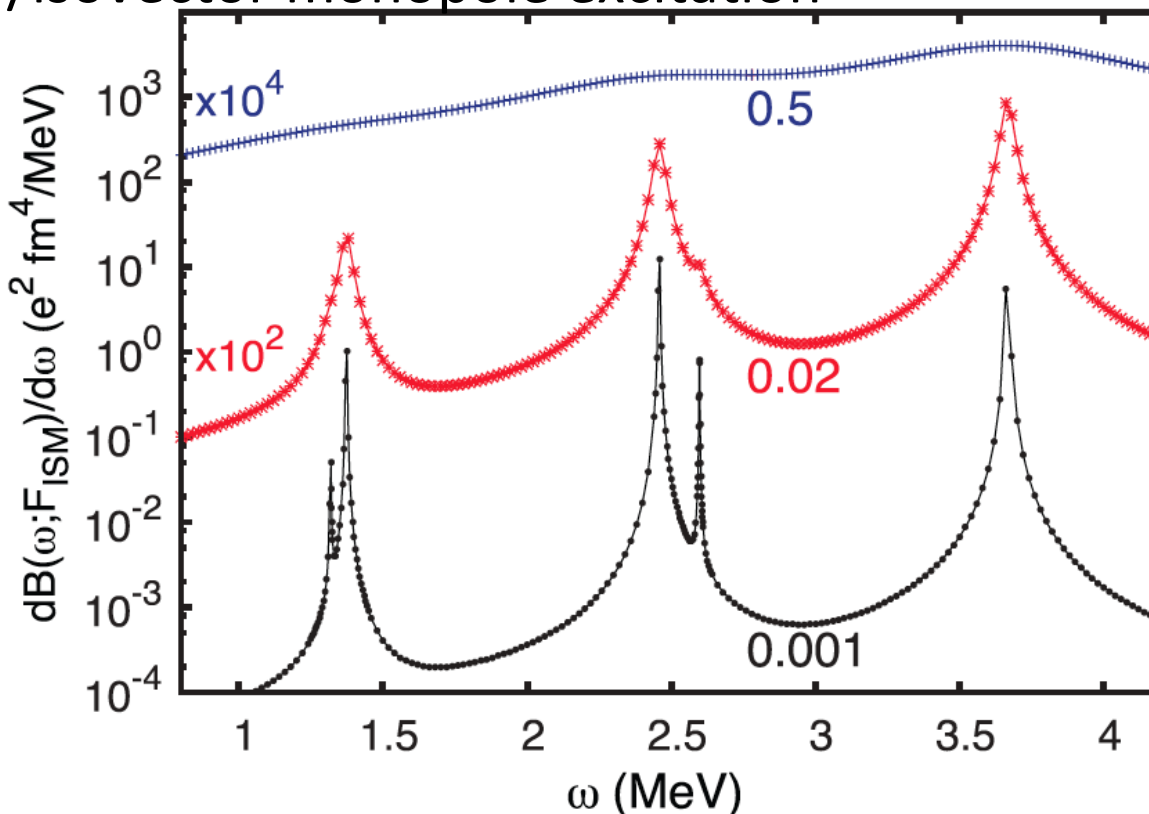


FIG. 1. (Color online) The low-lying isoscalar monopole strength at the oblate HFB minimum of ^{24}Mg calculated with the conventional FAM-QRPA using three values of smearing width γ (in MeV).

Numerical comparison with MQRPA (ISM)

24Mg, oblate, SLy4, Nsh=5, contour: circle, radius=0.02 MeV, discretized with 11 points

isoscalar monopole strength ($e^2 fm^4$)

Ω_i (MeV)				
MQRPA	FAM	MQRPA	FAM-C	FAM-D
1.3185	1.3183	5.729(-4)	5.776(-4)	5.781(-4)
1.3731	1.3731	1.539(-2)	1.510(-2)	1.511(-2)
2.4582	2.4581	0.1796	0.1784	0.1783
2.5998	2.5975	2.957(-3)	3.060(-3)	3.057(-3)
3.6687	3.6657	0.5776	0.5788	0.5788
5.1185	5.1212	3.539(-4)	4.360(-4)	4.345(-4)
7.4108	7.4084	0.4900	0.4848	0.4848

FAM: external field F dependent

complex-FAM derives QRPA amplitudes -- F independent eigenvectors

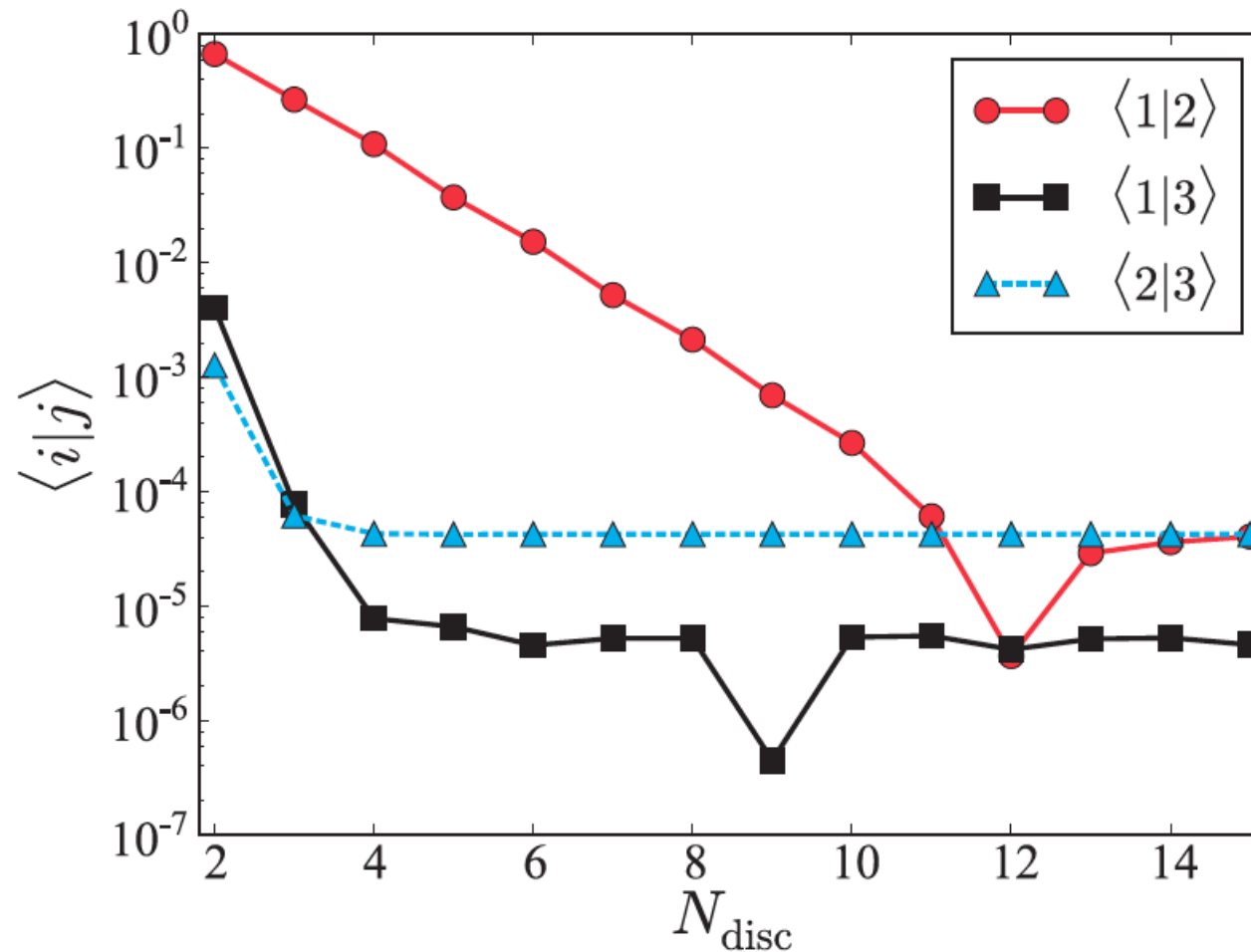
$$X_{\mu\nu}^i = e^{-i\theta} |\langle i | \hat{F} | 0 \rangle|^{-1} \frac{1}{2\pi i} \oint_{C_i} X_{\mu\nu}(\omega_\gamma) d\omega_\gamma,$$

$$\langle i | \hat{F} | 0 \rangle = \langle \Phi_0 | [\hat{O}_i, \hat{F}] | \Phi_0 \rangle = \sum_{\mu < \nu} (X_{\mu\nu}^{i*} F_{\mu\nu}^{20} + Y_{\mu\nu}^{i*} F_{\mu\nu}^{02})$$

$$Y_{\mu\nu}^i = e^{-i\theta} |\langle i | \hat{F} | 0 \rangle|^{-1} \frac{1}{2\pi i} \oint_{C_i} Y_{\mu\nu}(\omega_\gamma) d\omega_\gamma.$$

FAM-C: isoscalar operator, FAM-D: FAM from isovector operator

orthogonality of first three QRPA modes



1: 1.32 MeV, 2: 1.37 MeV, 3: 2.46 MeV

Rare-earth nuclei ($^{166,168,172}\text{Yb}$, ^{170}Er)

comparison with Vanderbilt code (SkM*)

MQRPA: Terasaki and Engel, PRC82, 034326 (2010), PRC84, 014332 (2011)

TABLE III. FAM-QRPA energies and $B(E2)$ values of the low-lying $K = 0$ states in ^{166}Yb , ^{168}Yb , ^{172}Yb , and ^{170}Er at $E_{\text{cut}} = 200$ MeV compared to the MQRPA results of Ref. [13]. The additional result for ^{172}Yb corresponding to $E_{\text{cut}} = 60$ MeV is compared to the MQRPA values obtained in Ref. [12].

Nucleus	Ω_i (MeV)		$B(E2)$ ($e^2 \text{ b}^2$)	
	MQRPA	FAM	MQRPA	FAM
^{166}Yb	1.802	1.422	0.0398	0.0327
^{168}Yb	2.039	1.747	0.0343	0.0186
^{172}Yb	1.605	1.306	0.0049	0.0088
^{170}Er	1.596	1.322	0.0030	0.0047
$^{172}\text{Yb}^{\text{a}}$	1.390	1.319	0.0050	0.0092

^a $E_{\text{cut}} = 60$ MeV.

radius: 0.1MeV, 0.02 MeV(^{168}Yb)
center: 1.40, 1.76, 1.30, 1.30MeV
 $^{166}\text{Yb}, 168\text{Yb}, 172\text{Yb}, 170\text{Er}$

	HFBTHO FAM	Vanderbilt MQRPA
HFB model space	N=20, 60, 200MeV cutoff	20fmx 20fm box, 60,200MeV cutoff
QRPA model space	full	cutoff associated with the occupation probabilities

Sum rules

sum rules

$$m_k(\hat{F}) = \sum_{\nu>0} \Omega_\nu^k |\langle \nu | \hat{F} | 0 \rangle|^2$$

- information of energy of giant resonances

$$E_k = \sqrt{\frac{m_k}{m_{k-2}}} \quad E_{-1} \leq E_0 \leq E_1 \leq \bar{E} \equiv \frac{m_1}{m_0} \leq E_2$$

- giant resonance width

$$\rho^2 \equiv E_2^2 - \bar{E}^2 \leq \frac{1}{4}(E_3^2 - E_1^2)$$

sum rule contains useful information of giant resonances

$$S(\hat{F}, \omega) = -2 \sum_{n=0}^{\infty} m_{-(2n+1)}(\hat{F}) \omega^{2n} \quad (|\omega| < \min_{\nu>0} \Omega_\nu) \quad S(\hat{F}, \omega) = 2 \sum_{n=0}^{\infty} \frac{m_{2n+1}(\hat{F})}{\omega^{2n+2}} \quad (|\omega| > \max_{\nu>0} \Omega_\nu)$$

contributions from all the excited states

- MQRPA

- HFB

- Thouless theorem($k=1, 3, \dots$ double commutator)

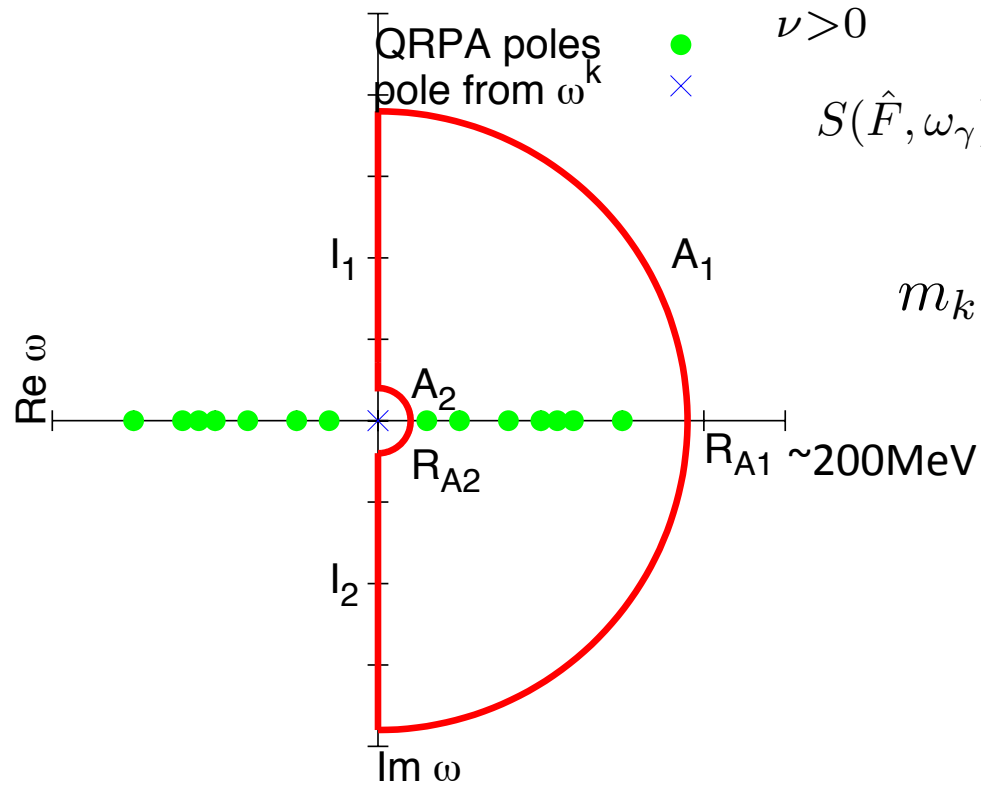
cannot be justified for DFT $m_1 = \sum_{\nu>0} \Omega_\nu |\langle \nu | \hat{F} | 0 \rangle|^2 = \frac{1}{2} \langle \text{HFB} | [\hat{F}, [\hat{H}, \hat{F}]] \text{HFB} \rangle$

- dielectric theorem for inverse energy weighted sum rule ($k=-1$)

Complex-energy FAM to QRPA sum rule

PRC91,044323 (2015)

□ QRPA sum rule $m_k(\hat{F}) = \sum_{\nu>0} \Omega_\nu^k |\langle \nu | \hat{F} | 0 \rangle|^2$



$$S(\hat{F}, \omega_\gamma) = - \sum_{\nu} \left\{ \frac{|\langle \nu | \hat{F} | 0 \rangle|^2}{\Omega_\nu - \omega_\gamma} + \frac{|\langle 0 | \hat{F} | \nu \rangle|^2}{\Omega_\nu + \omega_\gamma} \right\}$$

$$m_k = \frac{1}{2\pi i} \oint_D \omega_\gamma^k S(\hat{F}, \omega_\gamma) d\omega_\gamma$$

$$D = A_1 + I_1 + A_2 + I_2$$

Symmetries for hermitian operator: $k=1, 3, \dots$ contribution from A_1 only
 $k=-1$ (IWESR), contribution from A_2 only

- easily parallelized
- FAM along A_1 path converges rapidly with 5-6 iterations

Comparison with MQRPA/dielectric theorem

^{24}Mg oblate, Nsh=5

Sum rule, MQRPA / FAM, Isoscalar/Isovector monopole

TABLE V. Sum rules (in $\text{MeV}^k e^2 \text{ fm}^4$) for the isoscalar and isovector monopole operators calculated with the MQRPA and the FAM. The FAM calculations were performed by using $N_{A_1} = 301$, $N_{A_2} = 101$, and $N_{I_1} = 200$ integration points.

	$k = -4$	$k = -3$	$k = -2$	$k = -1$	$k = 0$	$k = 1$	$k = 2$	$k = 3$	$k = 4$
MQRPA(ISM)	0.013 077	0.037 185	0.253 118	5.00 072	139.825	4200.82	131 368	4 342 358	157 906 069
FAM(ISM)	0.012 579	0.036 992	0.253 186	5.00 385	139.844	4199.44	131 277	4 336 644	157 058 272
MQRPA(IVM)	0.00 063 616	0.00 273 872	0.07 120 949	2.78 540	113.908	4735.03	199 525	8 527 358	370 625 216
FAM(IVM)	0.00 043 157	0.00 275 227	0.07 133 510	2.78 615	113.908	4734.30	199 510	8 524 830	368 643 941

Dielectric theorem (HFB) for k=-1 sum rule

TABLE VII. Inverse-energy-weighted sum rule (in $\text{MeV}^{-1} e^2 \text{ fm}^4$) computed using the dielectric theorem (HFB) and the FAM for various sizes of the model space given by N_{sh} . FAM calculations were performed using $N_{A_2} = 22$ and $R_{A_2} = 1.0 \text{ MeV}$.

N_{sh}	FAM(ISM)	HFB(ISM)	FAM(IVM)	HFB(IVM)	FAM(ISQ)	HFB(ISQ)	FAM(IVQ)	HFB(IVQ)
5	5.00 385	5.00 375	2.78 615	2.78 614	4.44 830	4.44 765	0.798 680	0.798 680
10	11.2 033	11.2 102	5.09 467	5.09 671	5.21 547	5.21 586	1.07 516	1.07 524
15	12.4 930	12.5 009	5.71 677	5.71 960	5.31 250	5.31 268	1.12 916	1.12 910
20	12.9 506	12.9 634	6.06 842	6.07 304	5.35 499	5.35 730	1.15 744	1.15 771

Validity of Thouless theorem

TABLE VI. The energy weighted $K^\pi = 0^+$ sum rule (in MeV e^2 fm 4) for the operators (16)–(19) at the oblate minimum of ^{24}Mg as a function of N_{sh} . The FAM values were obtained by taking $R_{A_1} = 200$ MeV and $N_{A_1} = 12$; they are compared to HFB values (20). The results without time-odd terms except for the current-current coupling ($C_t^j \neq 0$ and $C_t^s(\rho_0) = C_t^{\Delta s} = C_t^{\nabla j} = C_t^T = 0$) (a) and with the full time-odd functional except for the current-current and kinetic spin-spin couplings ($C_t^T = C_t^{\nabla j} = 0$, $C_t^s(\rho_0) \neq 0$, $C_t^{\Delta s} \neq 0$, and $C_t^{\nabla j} \neq 0$) (b), obtained with $N_{\text{sh}} = 20$, are also listed.

N_{sh}	FAM(ISM)	HFB(ISM)	FAM(IVM)	HFB(IVM)	FAM(ISQ)	HFB(ISQ)	FAM(IVQ)	HFB(IVQ)
5	4199.44	4303.67	4734.25	4752.37	762.638	767.933	848.110	845.235
10	4524.39	4502.75	4970.34	4940.08	779.019	775.724	852.995	849.015
15	4521.39	4523.80	4958.02	4960.52	776.587	776.161	849.482	849.116
20	4530.01	4529.46	4966.98	4966.01	777.425	776.832	850.145	849.747
20 ^(a)	4530.07	–	4966.98	–	777.506	–	850.132	–
20 ^(b)	5297.64	–	5298.46	–	905.461	–	905.441	–

- Thouless theorem is satisfied in large model space
(enough size to express the coordinate operators in HO basis)
- Time-odd coupling constants are important to satisfy the theorem
(a): only C^j included, (b): C^j not included
- local gauge symmetry of $(\rho\tau-j^2)$ is necessary for these operators

Spontaneous symmetry breaking

- Nambu-Goldstone (NG) mode appears as a solution of self-consistent QRPA when mean field (DFT) breaks continuous symmetries which the original EDF has

broken symmetry	mean field	NG mode in the QRPA	K^π
translational (Galilean invariance)	center of mass fixed to the origin	center of mass motion	$0^-, 1^-$
rotational	deformation (axial or triaxial)	rotation	$1^+, (2^+)$
particle number (gauge symmetry)	pairing condensation (BCS)	pairing rotation	0^+
neutron-proton (isospin symmetry)	neutron-proton mixing	isospin rotation	0^+

NG mode restores the broken symmetry in the QRPA level

$$[\hat{H}_{\text{QRPA}}, \hat{\mathcal{P}}_{\text{NG}}] = i\Omega_{\text{NG}}^2 M_{\text{TV}} \hat{\mathcal{Q}}_{\text{NG}} = 0$$

$$[\hat{H}_{\text{QRPA}}, \hat{\mathcal{Q}}_{\text{NG}}] = -\frac{i}{M_{\text{TV}}} \hat{\mathcal{P}}_{\text{NG}}$$

\mathcal{P}_{NG} : broken symmetry (momentum operator)

Thouless-Valatin inertia from FAM

Phys. Rev. C92, 034321 (2015)

$$[\hat{H}_{\text{QRPA}}, \hat{Q}_{\text{NG}}] = -\frac{i}{M_{\text{TV}}} \hat{\mathcal{P}}_{\text{NG}}$$

M_{TV} : Thouless-Valatin inertia

Q_{NG} : canonical conjugate coordinate op.

Thouless-Valatin inertia from QRPA

$$M_{\text{TV}} = 2P_{\text{NG}}(A + B)^{-1}P_{\text{NG}}$$

FAM for NG modes:

Thouless-Valatin inertia is found from a linear response calculation at zero energy, using a broken-symmetry operator

$$S(\hat{\mathcal{P}}_{\text{NG}}, \omega = 0) = -M_{\text{TV}}$$

Thouless-Valatin inertia is found from the energy-weighted sum rule of the conjugate coordinate operator

$$M_{\text{TV}}^{-1} = 2m_1(\hat{Q}_{\text{NG}}) = \frac{2}{2\pi i} \int_D \omega S(\hat{Q}_{\text{NG}}, \omega) d\omega$$

Center of mass mode

trivial case

$$\hat{Q}_{\text{c.m.}} = \frac{1}{A} \sum_{i=1}^A \hat{r}_i, \quad \hat{P}_{\text{c.m.}} = -i \sum_{i=1}^A \hat{\nabla}_i$$

Thouless-Valatin inertia

$$M_{\text{CM}} = mA$$

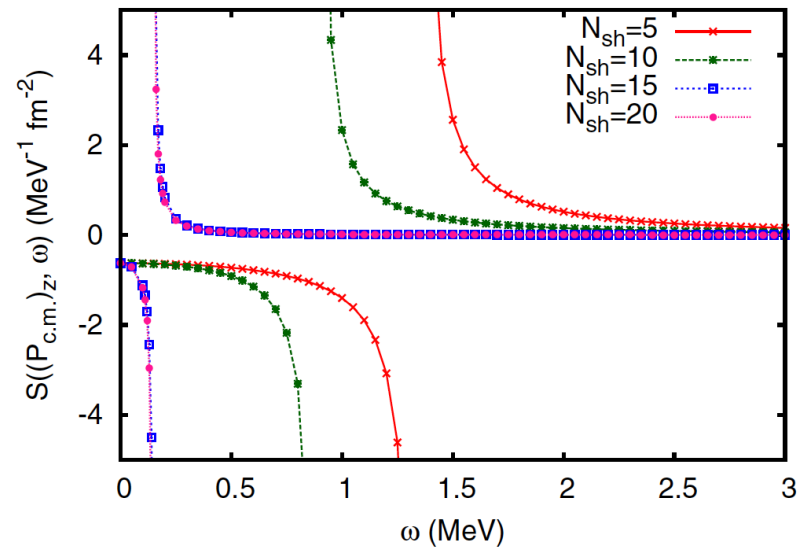
$$1/2m = A/2M_{\text{CM}}$$

finite HO basis:

translational mode is not at zero energy

$$S(\hat{P}_{\text{NG}}, \omega) \sim \frac{M_{\text{NG}} \Omega_{\text{NG}}^2}{\omega^2 - \Omega_{\text{NG}}^2}$$

$$\Omega_{\text{NG}}^2 = \frac{1}{S(\hat{P}_{\text{NG}}, 0) S(\hat{Q}_{\text{NG}}, 0)}$$

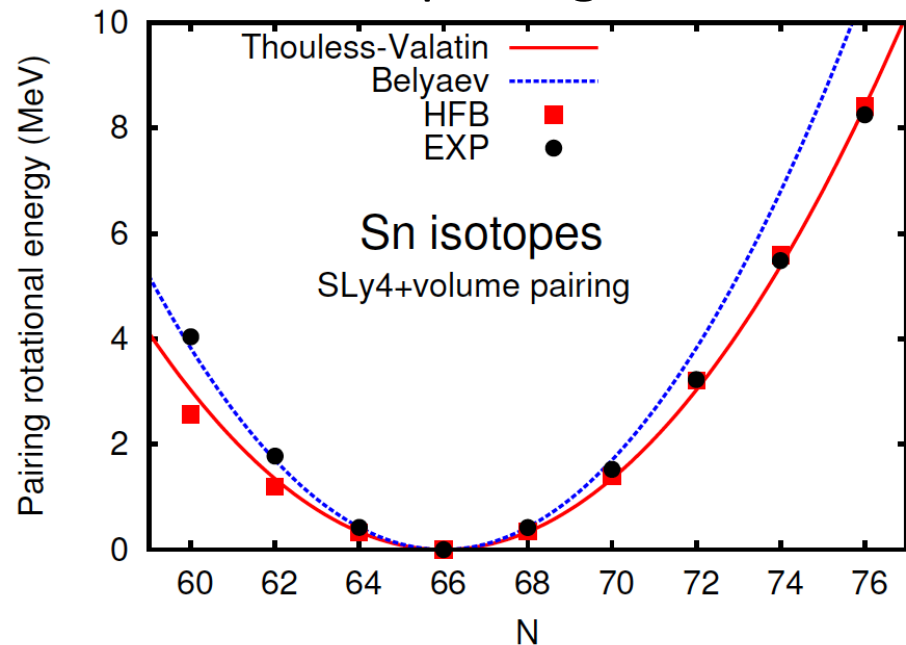


HFBTHO, SLy4+volume pairing, 26Mg (oblate)

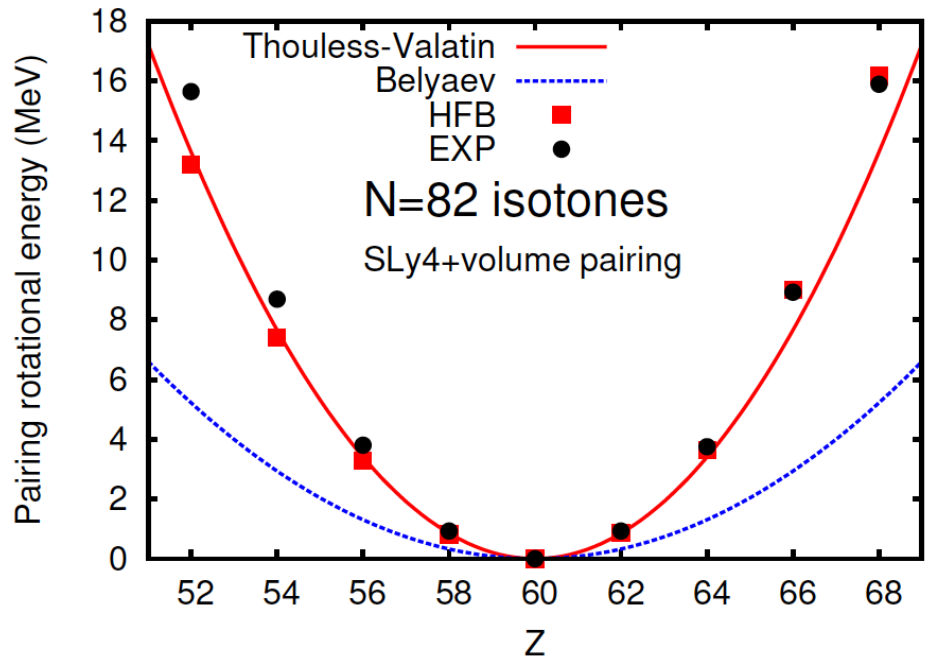
N_{sh}	$1/2m$ from $(\hat{Q}_{\text{c.m.}})_z$	$1/2m$ from $(\hat{P}_{\text{c.m.}})_z$	Inglis-Belyaev	$\Omega_{\text{c.m.}}$ MeV	$\langle [(\hat{Q}_{\text{c.m.}})_z, (\hat{P}_{\text{c.m.}})_z] \rangle / i$
5	20.69748	20.74676	26.04977	1.346	0.998836
10	20.78073	20.82140	25.87571	0.889	0.999310
15	20.73573	20.73232	25.73650	0.151	1.000026
20	20.73946	20.73666	25.74138	0.146	1.000041
exact	20.73553	20.73553		0	1

Neutron and proton pairing rotations

non-trivial case $\hat{\mathcal{P}}_{\text{NG}} = \hat{N}_n, \hat{N}_p$
 neutron pairing rotation



$\hat{\mathcal{Q}}_{\text{NG}} = \hat{\Theta}_n, \hat{\Theta}_p$ (unknown)
 proton pairing rotation



$$B(N, Z_0) = B(N_0, Z_0) + \lambda_n(N_0, Z_0)\Delta N + \frac{(\Delta N)^2}{2\mathcal{J}_n(N_0, Z_0)}$$

$\Delta N = N - 66$

pairing rotational energy

ground states form “pairing rotational bands”
 proton pairing: effect of residual Coulomb significant

Mixing of neutron and proton pairing rotations

when neutron and proton are in a superconducting phase

broken symmetries: neutron number and proton number

NG modes (QRPA eigenmodes): two, but mixing of two

TV inertias from two NG modes → three moments of inertia

QRPA eigenmodes

$$\hat{N}_1 = \hat{N}_n \cos \theta + \alpha \hat{N}_p \sin \theta,$$

$$\hat{\Theta}_1 = \hat{\Theta}_n \cos \theta + \frac{1}{\alpha} \hat{\Theta}_p \sin \theta$$

$$\hat{N}_2 = -\hat{N}_n \sin \theta + \alpha \hat{N}_p \cos \theta,$$

$$\hat{\Theta}_2 = -\hat{\Theta}_n \sin \theta + \frac{1}{\alpha} \hat{\Theta}_p \cos \theta$$

Thouless-Valatin mass of eigenmodes

$$M_1 = -S(\hat{N}_n, \hat{N}_n) \cos^2 \theta - \alpha^2 S(\hat{N}_p, \hat{N}_p) \sin^2 \theta \\ - 2\alpha S(\hat{N}_n, \hat{N}_p) \sin \theta \cos \theta,$$

$$M_2 = -S(\hat{N}_n, \hat{N}_n) \sin^2 \theta - \alpha^2 S(\hat{N}_p, \hat{N}_p) \cos^2 \theta \\ + 2\alpha S(\hat{N}_n, \hat{N}_p) \sin \theta \cos \theta,$$

$$S(\hat{N}_n, \hat{N}_n) = -2N_n(A+B)^{-1}N_n$$

$$S(\hat{N}_n, \hat{N}_p) = -2N_n(A+B)^{-1}N_p$$

$$S(\hat{N}_p, \hat{N}_p) = -2N_p(A+B)^{-1}N_p$$

constraint from orthogonality of two modes:

$$\tan 2\theta = \frac{2\alpha S(\hat{N}_n, \hat{N}_p)}{S(\hat{N}_n, \hat{N}_n) - \alpha^2 S(\hat{N}_p, \hat{N}_p)}$$

Mixing of neutron and proton pairing rotations

TV inertias from two NG modes → three moments of inertia

$$E_{\text{rot}}(N, Z) = \frac{(\Delta N_1)^2}{2M_1} + \frac{(\Delta N_2)^2}{2M_2},$$

$$= \frac{1}{2} (\Delta N - \Delta Z) \mathbb{J}^{-1} \begin{pmatrix} \Delta N \\ \Delta Z \end{pmatrix}$$

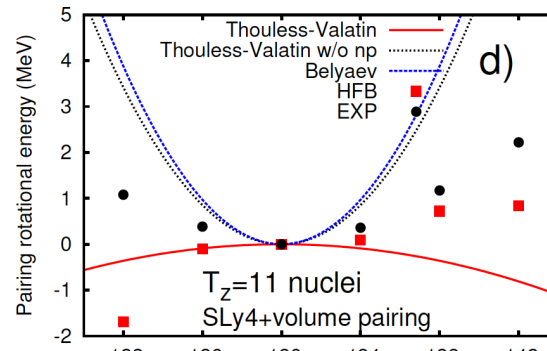
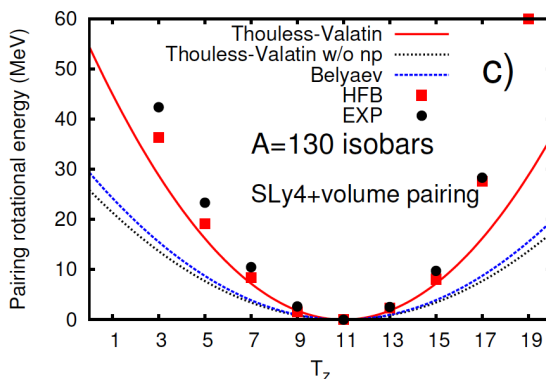
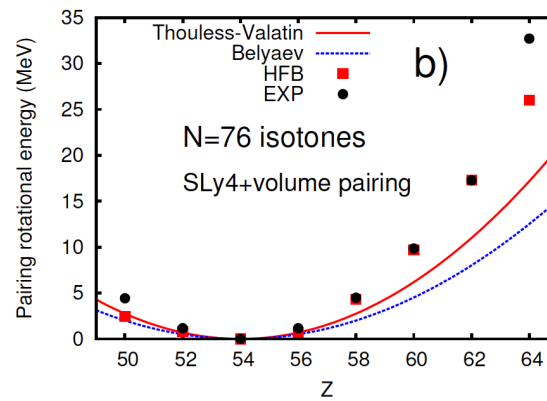
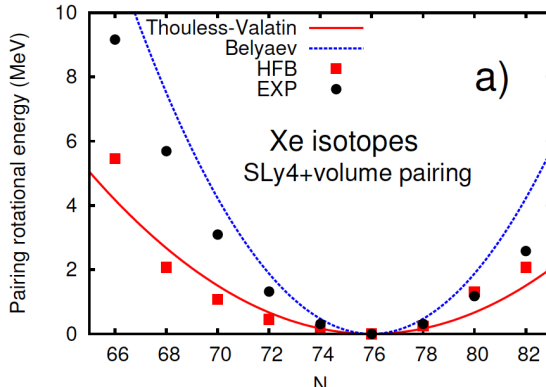
$$= \frac{(\Delta N)^2}{2\mathcal{J}_{nn}} + \frac{2(\Delta N)(\Delta Z)}{2\mathcal{J}_{np}} + \frac{(\Delta Z)^2}{2\mathcal{J}_{pp}}$$

inertia tensor

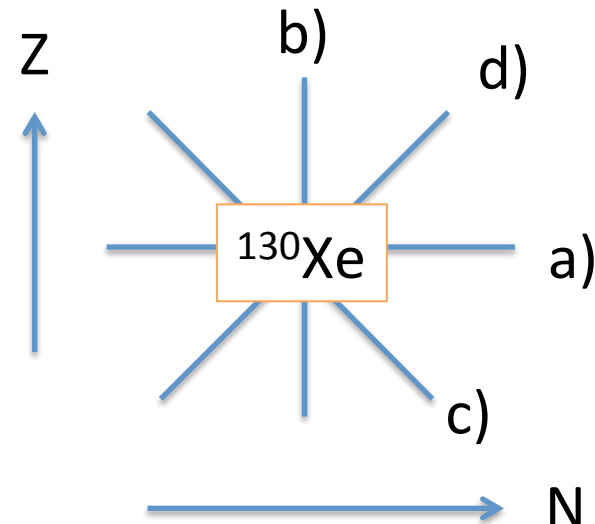
$$\mathbb{J}^{-1} = \begin{pmatrix} S(\hat{N}_n, \hat{N}_n) & S(\hat{N}_n, \hat{N}_p) \\ S(\hat{N}_p, \hat{N}_n) & S(\hat{N}_p, \hat{N}_p) \end{pmatrix}^{-1} = \begin{pmatrix} 1/\mathcal{J}_{nn} & 1/\mathcal{J}_{np} \\ 1/\mathcal{J}_{pn} & 1/\mathcal{J}_{pp} \end{pmatrix}$$

pairing rotation around

^{130}Xe nucleus



d): global gauge symmetry breaking^A, not associated with isovector pairing



Coordinate operator: spurious mode removal

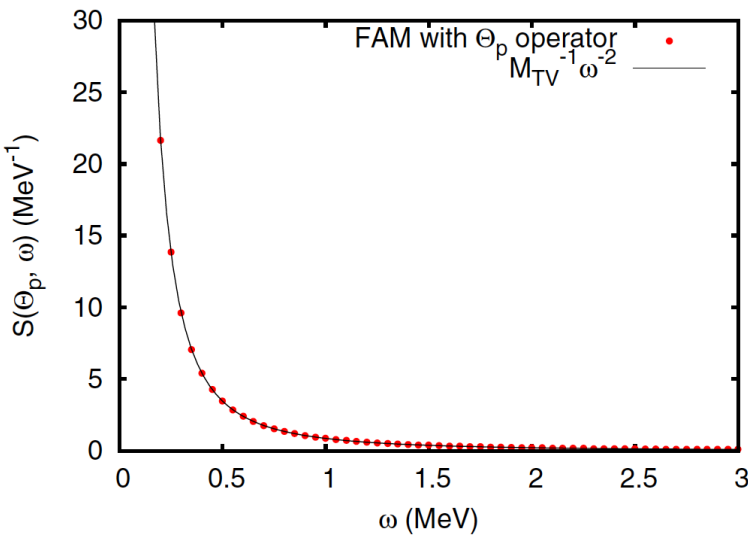
Conjugate coordinate operator (QRPA)

$$(A - B)Q_{\text{NG}}^R = \frac{P_{\text{NG}}^I}{M_{\text{NG}}}, \quad (A + B)Q_{\text{NG}}^I = -\frac{P_{\text{NG}}^R}{M_{\text{NG}}},$$

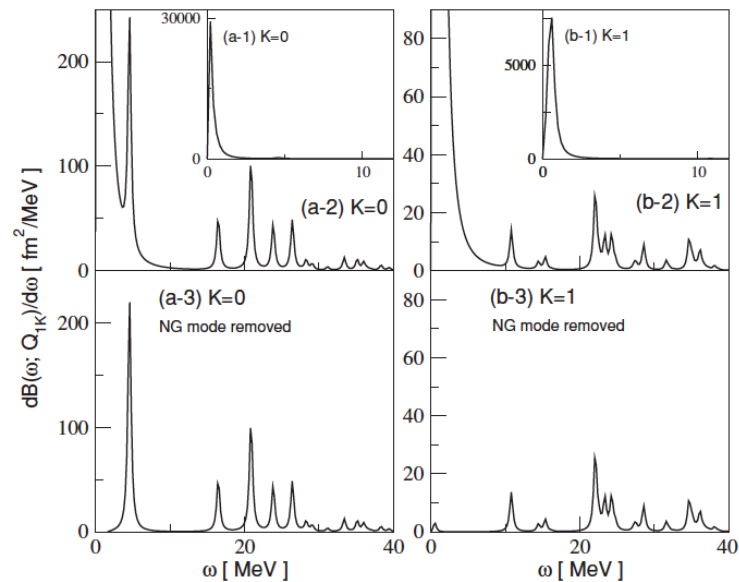
Conjugate coordinate operator (FAM)

$$Q_{\text{NG}} = -i \frac{X(0) + Y^*(0)}{2S(\hat{\mathcal{P}}_{\text{NG}}, 0)}$$

Pairing rotation



Rotation



Coordinate operator required for spurious mode removal (FAM/iterative Arnoldi)

$$\delta\rho_{\text{cal}}(\omega) = \delta\rho_{\text{phy}}(\omega) + \lambda_P \delta\rho_P + \lambda_R \delta\rho_R,$$

$$\delta\rho_R \equiv i[R, \rho_0] = \sum_i (|\bar{R}_i\rangle\langle\phi_i| + |\phi_i\rangle\langle\bar{R}_i|),$$

Nakatsukasa et al PRC76,024318(2007)

Non-axial ($K \neq 0$) QRPA modes with axial HFBTHO

Kortelainen,NH,Nazarewicz arXiv:1509.02353.

explicit linearization necessary for density-dependent term

$$\delta\rho(\omega) = \frac{\rho_\eta - \rho_0}{\eta} + O(\eta^2)$$

$$\delta\kappa^{(\pm)}(\omega) = \frac{\kappa_\eta^{(\pm)} - \kappa_0}{\eta} + O(\eta^2)$$

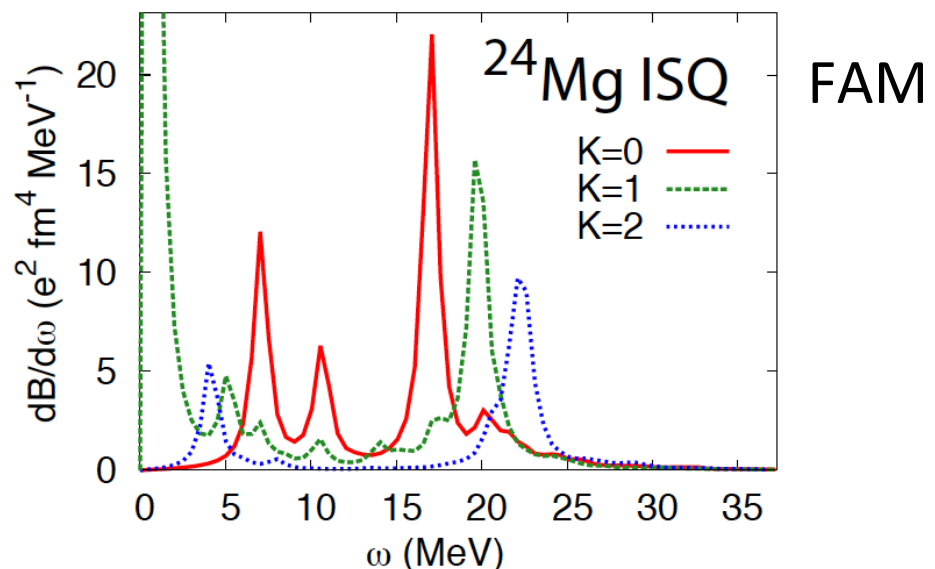
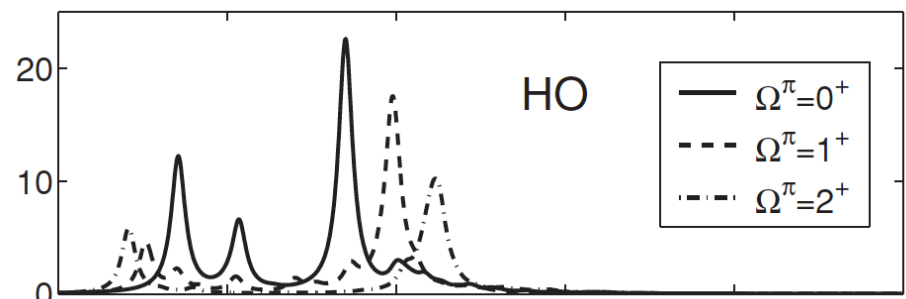
$$\delta h(\omega) = \frac{h[\rho_\eta, \kappa_\eta^{(+)}, \kappa_\eta^{(-)*}] - h[\rho, \kappa, \kappa^*]}{\eta},$$

$$\delta\Delta^{(+)}(\omega) = \frac{\Delta[\rho_\eta, \kappa_\eta^{(+)}, \kappa_\eta^{(-)*}] - \Delta[\rho, \kappa, \kappa^*]}{\eta},$$

$$\delta\Delta^{(-)}(\omega) = \frac{\Delta[\rho_\eta^\dagger, \kappa_\eta^{(-)}, \kappa_\eta^{(+)*}] - \Delta[\rho, \kappa, \kappa^*]}{\eta},$$

MQRPA

(Losa et al.PRC81, 064307(2010))

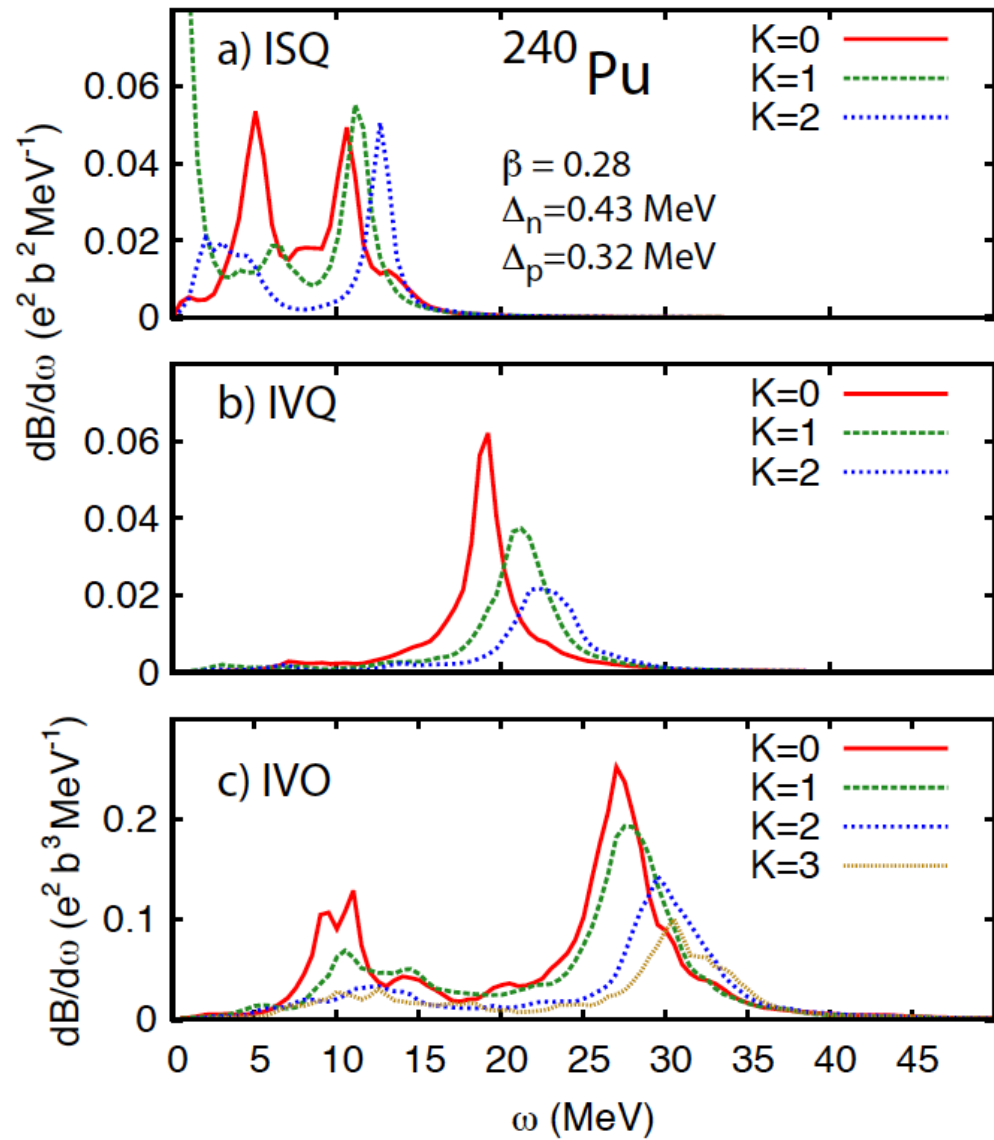
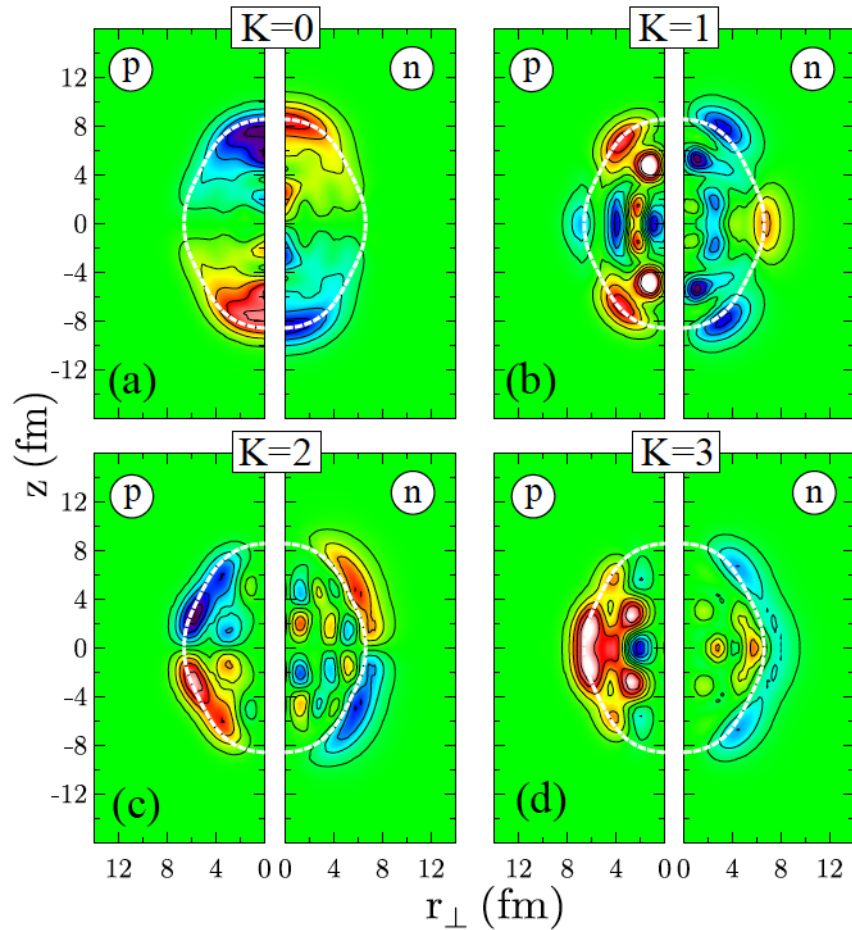


^{240}Pu quadrupole/octupole modes

SLy4 + mixed pairing, $N_{\text{sh}}=20$

transition amplitudes

IVO, $\omega=11$ MeV



^{154}Sm low-lying octupole vibration

SLy4 + mixed pairing

TABLE I. Lowest octupole QRPA modes in ^{154}Sm predicted in our deformed FAM calculations. Shown are: the energy ω_1 ; the IVO transition strength $|\langle 0|f_{L=3,K}^{IV,+}|1\rangle|^2$; and the corresponding $B(\text{E3})$ value. The transition probabilities were computed through the QRPA amplitudes (referred to as FAM-C in [27]).

K	ω_1 (MeV)	$ \langle 0 f_{L=3,K}^{IV,+} 1\rangle ^2$ ($e^2\text{fm}^6 \text{ MeV}^{-1}$)	$B(\text{E3})$ (W.u.)
0	0.4168	6.684	8.70
1	0.9014	69.74	2.01
2	2.5973	1.916	0.24
3	1.3155	0.01809	0.0004

Experimental data:

$K=0$ 0.9213 MeV $B(\text{E3})$: 10(2) W.u.

$K=1$ 1.4758 MeV

Summary

Recent development of finite-amplitude method

- discrete collective modes
- sum rules
- Nambu-Goldstone mode, Thouless-Valatin inertia
- non-axial response

Outlook

- systematic calculation of nuclear responses
- DFT optimization using information on excitation
- 2+ energy systematics /pairing rotations

Collaborators

- Markus Kortelainen (Jyvaskyla, Finland)
- Witold Nazarewicz (MSU, USA)
- Erik Olsen (MSU, USA)

Calculations

HPCC, iCER, MSU



COMA(PACS-IX), Tsukuba

